Short Communication: Monitoring rock falls with the Raspberry Shakes

Andrea Manconi[1*], Velio Coviello[2], Maud Galletti[1], Reto Seifert[1]

[1]Swiss Federal Institute of Technology, Dept. of Earth Sciences, Zurich, 8092, Switzerland
5   [2]Free University of Bozen-Bolzano, Facoltà di Scienze e Tecnologie, Italy

Correspondence to: A. Manconi (andrea.manconi@erdw.ethz.ch)

Abstract. We evaluate the performance of the low-cost seismic sensors Raspberry Shake (RS) to identify and monitor rock fall activity in alpine environments. The test area is a slope adjacent to the Great Aletsch glacier in the Swiss Alps, i.e. the
10   Moosfluh deep-seated instability, which is undergoing an acceleration phase since the late summer 2016. A local seismic network composed of three RS seismometers was deployed starting from May 2017, in order to record rock fall activity and its relation with the progressive rock slope degradation potentially leading to a large rock slope failure. Here we present a first assessment of the seismic data acquired from RS sensors after a monitoring period of 1-year. A webcam was installed on the opposite side of the active slope, acquiring images every 10 minutes to validate the occurrence and identify rock falls
15   as well as their location and approximate size. Despite seismic data were collected mainly to identify rock fall phenomena, other event types were recorded during the monitoring period. Thus, this work provides also general insights on the potential use of low cost sensors in environmental seismology investigations.

1 Introduction

Rock falls constitute a major hazard in most steep natural rock slopes. The growing number of residential buildings and
20   transport infrastructures in mountain areas has progressively increased the exposure to such processes, making the development of reliable detection systems crucial for early warning and rapid response (Stähli et al., 2015). Local geological and geomorphological conditions are the main pre-disposing factors affecting the sizes of failing rock blocks, the falling dynamics, as well as the total run out distances (Corominas et al., 2017). Different triggering agents (mainly earthquakes and/or meteo-climatic variables) have also an impact on of slope failure processes, which can range from a single block fall
25   scenario to large and more complex rock avalanches. In addition, increase of rock fall activity has been observed in areas affected by large and deep seated slope instabilities prior to catastrophic failure events (Rosser et al., 2007).

Accurate catalogues (including event location, time, and magnitude) are essential to understand and forecast rock falls, as well as other landslide processes (Kirschbaum et al., 2010). Usual approaches to build catalogues are based on chronicles and observations of past events; however, catalogues may lack of completeness, as the information is often qualitative,
30   arbitrary, and constrained to limited time windows and/or specific locations. This is especially true for small- to medium-size

rock fall events (e.g., Paranunzio et al., 2016). For this reasons, there is an increasing focus on quantitative monitoring approaches, which can provide more accurate and unbiased datasets. In this context, different monitoring sensor types can be considered, ranging from ground-based and remote systems. Ground-based detection systems are based on in-situ networks composed of instruments installed on the unstable rock slopes (such as for example extensometers), in order to catch

5 precursory changes of rock mass damage eventually leading to failure. Despite, they are often difficult to install and maintain in alpine areas mainly for logistical reasoning. Moreover, prior knowledge of the geological, geomorphological, and historical predisposing factors is necessary for their installation, and this is possible only for relatively small and constrained areas. On the other hand, remote detection systems are here defined as instruments and techniques used to monitor physical changes of the rock slope/wall surface from a distance. Photogrammetric techniques, laser scanning, and radar interferometry

10 are the most employed remote detection systems, considering regular surveys in the study areas to detect any diachronic change in the rock surface characteristics (Strozzi et al., 2010). These techniques are typically applied considering both ground-based and airborne platforms (airplane, helicopter, UAVs), while space-borne data is not currently suitable due to spatial and temporal resolution incompatible with the analysis of rock fall processes (Manconi et al., 2018). Compared with classical in-situ techniques, remote systems can be employed at a safe distance from the unstable slope; however, they are

15 often difficult to adapt to specific site conditions in mountain regions (difficult access to the monitoring site, low visibility of the slope to monitor, meteorological conditions, high costs). In addition, continuous monitoring settings are still rare, thus also hindering the possibility to generate complete rock fall catalogues.

Rock fall phenomena induce also seismic waves (e.g., Dammeier et al., 2011; Dietze et al., 2017). Seismic instruments can be installed directly on the unstable rock face to catch precursory signs of rock failure (Arosio et al., 2009), or at relatively

20 large distances to detect a rock fall event occurrence and its propagation (Manconi et al., 2016). In particular, seismic sensors present a significant number of advantages compared to other sensors as they are (i) compact, relatively low-cost sensors, (ii) highly adaptable to difficult field conditions, (iii) and can provide reliable information in their flat-response frequency range on a broad spectrum of mass wasting processes occurring in relatively large areas (Burtin et al., 2014; Coviello et al., 2015). Consequently, in recent years the seismic signature of rock slope failure phenomena has been investigated by several authors

25 in different environments and monitoring set-ups (e.g., Helmstetter and Garambois, 2010; Zimmer and Sitar, 2015). The results have shown how from the seismic signals is possible to derive information to characterize rock falls, with different level of accuracy depending upon signal sampling rates, distances between the sensors and the event, as well as the network density. The latter parameter is associated to the available budget for monitoring, thus low-cost solutions are becoming more and more attractive to increase the capability of detection and investigation of seismic activity (Cochran, 2018).

30 In this short communication, we show the initial results of a pilot project testing a recently developed low-cost seismic sensor, i.e. the Raspberry Shake seismometer, aiming at following the evolution of rock slope damage associated to a large, deep-seated slope instability located in the Swiss Alps. In the following sections, we provide a short technical description of the sensor, introduce the study area selected, and describe the results obtained after 1-year of continuous monitoring.

2 The Raspberry Shake

The Raspberry Shake is an all-in-one, IoT plug-and-go solution for seismological applications. Developed by OSOP, S.A. in Panamá, the Raspberry Shake integrates the geophone sensors, 24-bit digitizers, period-extension circuits and computer into a single enclosure. The signal detected by a 4.5 Hz 380-400 Ohm geophone goes to an analogue system where it is amplified and period-extended from the geophone's natural frequency of 4.5 Hz down to 2 seconds, thus providing improved signal bandwidth at lower frequencies essential for earthquake detection. The analogue signal is then digitized with a 24-bit analogue-to-digitizer (ADC) converter at 800 samples per second (sps). Then, the signal is down sampled to 100 sps through a series of anti-aliasing routines. The -3 dB points that define the digital signal output bandwidth are estimated at 80% of Nyquist, or 40 Hz, and 2 seconds (see Supplementary Information, Figure S1)

The minimum detection threshold is estimated at 0.03 μm/s RMS from 1 to 20 Hz at 100 sps where the minimum detectable level is considered to be 10 dB above the noise RMS. Dynamic range is the full-scale sinusoid RMS over the noise RMS in dB. The dynamic range for the entire sensor is estimated to be 21 bits (126 dB) from 1 to 20 Hz at 100 sps. The instrument self-noise is, therefore, suited for local, regional and teleseismic earthquake detection (see Supplementary information, Figure S2). The Raspberry Shake is compatible with all standards in earthquake seismology: data are transmitted in from a native SEEDlink server running on a Debian OS in miniSEED format and can be ingested directly into most mainstream data processing software packages without modification.

3 Area of study and monitoring network

The Great Aletsch Region (Swiss Alps, see Figure 1) has undergone to several cycles of glacial advancement and retreat, which have deeply affected the evolution of the surrounding landscape (Grämiger et al., 2017). Currently, this region is one of the places where the effects of climate change can be strikingly observed, as the Aletsch glacier (blue shading in Fig. 1) is experiencing remarkable retreat with rates in the order of 50 meters every year (Jouvet et al., 2011). In particular, a deep-seated slope instability located in the southern slope of the Aletsch valley, more specifically in the area called "Moosfluh", has shown during the past decades years evidences of progressive increase of surface displacement (Kos et al., 2016; Strozzi et al., 2010). In the late summer 2016, an unusual acceleration of the Moosfluh rockslide was observed, with maximum velocities reaching locally up to 1 meter per day (Manconi et al., 2018). Such a critical evolution caused the generation of deep tensile cracks, and resulted in an increased number of rock failures at different locations of the landside body. In this scenario, we have installed a local network composed of three RS sensors of the M9 type (vertical component only, 50 Hz sampling rate, see location in Figure 1 a-c). RS-1 (installed on May 19, 2017) and RS-2 (installed on June 27, 2017) are co-located within precedent monitoring infrastructures and exploit from there the necessary power (solar panels and batteries) and the internet connection (GSM) necessary for real time data transmission (Loew et al., 2017). RS-3 (installed on July 03, 2017) is located in the basement of the Moosfluh cable car station, and leverages from existing power and Internet connection facilities. The coupling between the station and the ground is granted through a metal plate screwed directly on

the rock face, and a fiberglass protection was used to provide isolation from direct effects external agents (rain, snow, dust, animals, etc.). Compared with RS-1 and RS-2, the data acquired at RS-3 is affected from a higher level of noise during the cable car operational time period (between 8am and 4.30pm local time); however, we aimed at testing the potential detection of signals associated with rock falls in such a scenario highly affected by anthropic seismic noise. Data acquired from RS-1

5 and RS-2 is transmitted in real-time to the ETH Zurich servers via GSM network through a mobile access router (AnyRover, see details at www.anyweb.ch). Instead, the RS-3 data is stored locally and also transmitted to a Winston Wave Server (WWS, caps.raspberryshakedata.com). A Mobotix M25 webcam (5Mpixel resolution) is installed at the RS-1 location and acquires pictures every 10 minutes (Manconi et al., 2018). The use of optical data acquired from the webcam is mainly aimed at validating (during day light, cloud-free conditions) the effective occurrence of rock fall phenomena when signals

10 are detected in the seismic waveforms. RS-1 and RS-2 stations, both installed on the ground surface at elevations >2,000 m a.s.l. in an alpine environment, provided continuous record of seismic data since the installation without any site intervention in the 1-year monitoring period presented here. Air temperatures in this period ranged from -20 degrees in winter to +25 degrees in summer, and snow cover up to 3 meters was recorded at the RS-2 location and around 1.5 meters at RS-1 location between January and March 2018.

4 Preliminary results

4.1 Earthquakes

In a monitoring scenario where the main interest is to detect rock falls, recognition of earthquake events in the seismic traces is very important for two main reasons: (i) ground shaking due to local earthquakes (distances <100 km) can cause rock falls (Romeo et al., 2017), thus their identification is important to properly study the triggering factors affecting the rock slope

20 degradation; (ii) the signals associated to distant events, such as regional earthquakes (distance >100 km) and teleseisms (distance >1000 km) have characteristics that might be similar (in terms of amplitudes and durations) with the signals due to mass wasting phenomena (Dammeier et al., 2011; Helmstetter and Garambois, 2010; Manconi et al., 2016), and thus introduce a bias in the aimed rock fall catalogue. In order to test the performance of our local RS network, we selected 65 seismic events from the catalogue provided by USGS (NEIC), considering crustal events at depths lower than 50 km,

25 magnitudes larger than M2.5, and occurred at distances up to 15,000 km from our study area within 1-year time period (May 19, 2017 and May 19, 2018). Then, we processed the data acquired by the station RS-1 to automatically generate a catalogue of events. We band-pass filtered the RS-1 signal between 0.5 and 15 Hz, and applied the STA/LTA event detector implemented in the GISMO software suite (Reyes and West, 2011). Finally, we searched for matches between our RS-1 catalogue and the reference earthquake catalogue, considering an approximated P-wave travel time scaling relationship. We

30 found a match for 47 out of the 65 earthquake events (~73%). In Figure 2a, we show the spatial distribution of the recorded earthquakes. As expected, the detectable magnitude as well as the signal amplitude scales with the distance from the seismic

event's source. From the waveforms (Figure 2 c-f) it is possible to recognize the main differences in terms of amplitudes, duration and signal characteristics for different events.

4.2 Rock fall signals

A number of 250 rock fall events have been identified in the period between 1 July and 31 October 2017, and the majority of them occurred over night (see Supplementary Information, Figure S3). In Figures 3 we show a selection of those events to provide an insight on the potential use of RS sensors for this specific monitoring activity. Qualitative analysis on the signals recorded by the three stations already provides preliminary indications on the rock fall processes. Considering the amplitudes and durations of the waveforms, we can derive first-order interpretations on the size of the rock fall and/or on the complexity of the event. For example, the rock fall signal recorded on 21 August, 2017 is very different from the one acquired on 19 September 2017 in terms of maximum amplitude and total duration. Indeed, the first one is associated to the failure of a single block that, however, did not run out very long due to low energy and/or unfavourable kinematic conditions (presence of obstacles, such as deep counterscarps present in the Moosfluh area), while the second is associated to a relatively large rock avalanche involving several rock blocks with some of them reaching the glacier. In general, the RS-2 station, which is located on the same slope affected by the rock failure at ~1km distance from the source area, presents larger amplitudes compared to RS-1 (located in front of the rock fall area on the other side of the valley) and to RS-3 (installed a the cable car location). This is always true for the relatively small rock falls, while in case of events with longer durations (see for example the 19 September, 2017 event in Figure 3) RS-3 records the largest amplitude. On the other hand, a signal recorded on August 23, 2017 (see Supplementary Information, Figure S4) presents typical characteristics of a surficial mass wasting, i.e. emerging onset and major spectral content between 2 and 5Hz; however, the first arrivals as well as the amplitudes are very similar at both RS-1 and RS-2 (high noise levels due to the cable car operations do not allow detect this event at RS-3). Moreover, the webcam pictures acquired before and after the event do not show changes that are potentially referred to a mass wasting in the local study area. This indicates that the event likely occurred outside our RS network. Indeed, this signal is the seismic signature of the Piz Cengalo rock avalanche (ca. 3 million cubic meters of failed material) occurred more than 100 km away from the monitoring location (Amann et al., 2018). This shows the potential of RS stations to measure relatively large surface mass wasting processes at regional scales.

The webcam pictures helped to confirm events recorded during day light, cloud-free conditions; however, as the majority of the events in our period of observation occurred over night (see Figure S3), the identification is often not straightforward when there is more than one event per night. In Figure 4, we show a clear example where the seismic signals recorded at the three RS stations is validated as a rock fall event by coeval pictures. In other cases, however, clear seismic signals are not associated to changes detectable in the webcam pictures. This can be caused by lack in the pictures resolution and/or by rock fall events occurred out from the camera footprint, as well as by other processes occurring in the subsurface (Poli et al., 2017).

4.3 Other sources of seismic signals

A part from geophysical phenomena, we have also recorded seismic signals associated to environmental variables (such as rainfall events), anthropic nature (for example helicopter and airplane flights) and/or of unclear source (see Supplementary Information, Figure S5). RS-1 and RS-2 are installed at the ground surface, thus more exposed to local noise sources.
5   Moreover, they are unprotected from daily and seasonal temperature variations, which can cause additional disturbances to the seismic records. In the supplementary information we report examples of these signals. Future work is aimed at exploring ad-hoc algorithms to attempt automatic detection and location of the rock fall events in this specific setting, thus other sources of seismic signals will be further investigated to better understand their nature and mitigate their effect on our data analysis.

10   ## 5. Summary

High-resolution, dense seismic networks are expensive to install and need resource-intense maintenance: one high-resolution seismic station costs in the order of tens of thousands dollars to build and equip, including sensors, on-site data acquisition systems, telecommunications, and back-up power (Cochran, 2018). In this short communication we show the preliminary results of a pilot project aimed at testing low-cost seismic sensors to detect and monitor the spatial and temporal evolution of
15   rock slope damage in the area of Moosfluh. We have installed a local network composed of three Raspberry Shake M9 seismometers and acquired continuously data for a period of 1-year. Seismic data acquired from RS sensors allowed to discriminate between rock fall events associated to the evolution of slope instability, e.g., rock fall phenomena of different size and run out, and seismic events, such as regional earthquakes and teleseisms. Our first assessment provides hints for the use of low cost sensors to increase the spatial and temporal acquisition of rock fall phenomena in alpine areas.
20

References

Amann, F., Kos, A. , Phillips, M. Kenner, R.: The Piz Cengalo Bergsturz and subsequent debris flows, Geophysical Research Abstracts, Vol. 20, EGU2018-14700, 2018
Arosio, D., Longoni, L., Papini, M., Scaioni, M., Zanzi, L. and Alba, M.: Towards rockfall forecasting through observing
30   deformations and listening to microseismic emissions, Nat. Hazards Earth Syst. Sci., 9, 1119–1131, 2009.

Burtin, A., Hovius, N., McArdell, B. W., Turowski, J. M. and Vergne, J.: Seismic constraints on dynamic links between geomorphic processes and routing of sediment in a steep mountain catchment, Earth Surf. Dyn., 2(1), 21–33, doi:10.5194/esurf-2-21-2014, 2014.

Cochran, E. S.: To catch a quake, Nat. Commun., 9(1), 2508, doi:10.1038/s41467-018-04790-9, 2018.

5 Corominas, J., Mavrouli, O. and Ruiz-Carulla, R.: Magnitude and frequency relations: are there geological constraints to the rockfall size?, Landslides, doi:10.1007/s10346-017-0910-z, 2017.

Coviello, V., Arattano, M. and Turconi, L.: Detecting torrential processes from a distance with a seismic monitoring network, Nat. Hazards, 78(3), 2055–2080, doi:10.1007/s11069-015-1819-2, 2015.

Dammeier, F., Moore, J. R., Haslinger, F. and Loew, S.: Characterization of alpine rockslides using statistical analysis of

10 seismic signals, J. Geophys. Res., 116(F4), F04024, doi:10.1029/2011JF002037, 2011.

Dietze, M., Mohadjer, S., Turowski, J. M., Ehlers, T. A. and Hovius, N.: Seismic monitoring of small alpine rockfalls – validity , precision and limitations, Earth Surf. Dyn., 5, 653–668, 2017.

Grämiger, L. M., Moore, J. R., Gischig, V. S., Ivy-Ochs, S. and Loew, S.: Beyond debuttressing: Mechanics of paraglacial rock slope damage during repeat glacial cycles, J. Geophys. Res. Earth Surf., 2016JF003967, doi:10.1002/2016JF003967,

15 2017.

Helmstetter, A. and Garambois, S.: Seismic monitoring of Séchilienne rockslide (French Alps): Analysis of seismic signals and their correlation with rainfalls, J. Geophys. Res., 115(F3), F03016, doi:10.1029/2009JF001532, 2010.

Jouvet, G., Huss, M., Funk, M. and Blatter, H.: Modelling the retreat of Grosser Aletschgletscher, Switzerland, in a changing climate, J. Glaciol., 57(206), 1033–1045, 2011.

20 Kirschbaum, D. B., Adler, R., Hong, Y., Hill, S. and Lerner-Lam, A. L.: A global landslide catalog for hazard applications—Method, results, and limitations, Nat. Hazards, 52, 561–575, doi:10.1007/s11069-009-9401-4, 2010.

Kos, A., Amann, F., Strozzi, T., Delaloye, R., von Ruette, J. and Springman, S.: Contemporary glacier retreat triggers a rapid landslide response, Great Aletsch Glacier, Switzerland, Geophys. Res. Lett., 2016GL071708, doi:10.1002/2016GL071708, 2016.

25 Loew, S., Gischig, V., Glueer, F., Seifert, R. and Moore, J. R.: Multidisciplinary monitoring of progressive failure processes in brittle rock slopes, in Rock Mechanics and Engineering Volume 4: Excavation, Support and Monitoring, vol. 4, pp. 629–662, CRC Press, London., 2017.

Manconi, A., Picozzi, M., Coviello, V., De Santis, F. and Elia, L.: Real-time detection, location, and characterization of rockslides using broadband regional seismic networks, Geophys. Res. Lett., 43(13), 6960–6967,

30 doi:10.1002/2016GL069572, 2016.

Manconi, A., Kourkouli, P., Caduff, R., Strozzi, T. and Loew, S.: Monitoring Surface Deformation over a Failing Rock Slope with the ESA Sentinels: Insights from Moosfluh Instability, Swiss Alps, Remote Sens., 10, doi:10.3390/rs10050672, 2018.

Paranunzio, R., Laio, F., Chiarle, M., Nigrelli, G. and Guzzetti, F.: Climate anomalies associated to the occurrence of

rockfalls at high-elevation in the Italian Alps, Nat. Hazards Earth Syst. Sci., 2016(16), 2085–2106, doi:10.5194/nhess-2016-100, 2016.

Poli, P.: Creep and slip: Seismic precursors to the Nuugaatsiaq landslide (Greenland), Geophys. Res. Lett., 44, 8832–8836, doi:10.1002/2017GL075039, 2017.

5   Reyes, C. G. and West, M. E.: The Waveform Suite: A Robust Platform for Manipulating Waveforms in MATLAB, Seismol. Res. Lett., 82(1), 104–110, doi:10.1785/gssrl.82.1.104, 2011.

Romeo, S., Matteo, L. Di, Melelli, L., Cencetti, C., Dragoni, W. and Fredduzzi, A.: Seismic-induced rockfalls and landslide dam following the October 30, 2016 earthquake in Central Italy, Landslides, 1–9, doi:10.1007/s10346-017-0841-8, 2017.

Rosser, N., Lim, M., Petley, D., Dunning, S. and Allison, R.: Patterns of precursory rockfall prior to slope failure, J.

10   Geophys. Res. Earth Surf., 112(F4), F04014, doi:10.1029/2006JF000642, 2007.

Stähli, M., Sättele, M., Huggel, C., McArdell, B. W., Lehmann, P., Van Herwijnen, a., Berne, a., Schleiss, M., Ferrari, a., Kos, a., Or, D. and Springman, S. M.: Monitoring and prediction in early warning systems for rapid mass movements, Nat. Hazards Earth Syst. Sci., 15(4), 905–917, doi:10.5194/nhess-15-905-2015, 2015.

Strozzi, T., Delaloye, R., Kääb, A., Ambrosi, C., Perruchoud, E. and Wegmüller, U.: Combined observations of rock mass

15   movements using satellite SAR interferometry, differential GPS, airborne digital photogrammetry, and airborne photography interpretation, J. Geophys. Res., 115(F1), doi:10.1029/2009JF001311, 2010.

Zimmer, V. L. and Sitar, N.: Detection and location of rock falls using seismic and infrasound sensors, Eng. Geol., 193, 49–60, doi:10.1016/j.enggeo.2015.04.007, 2015.

20
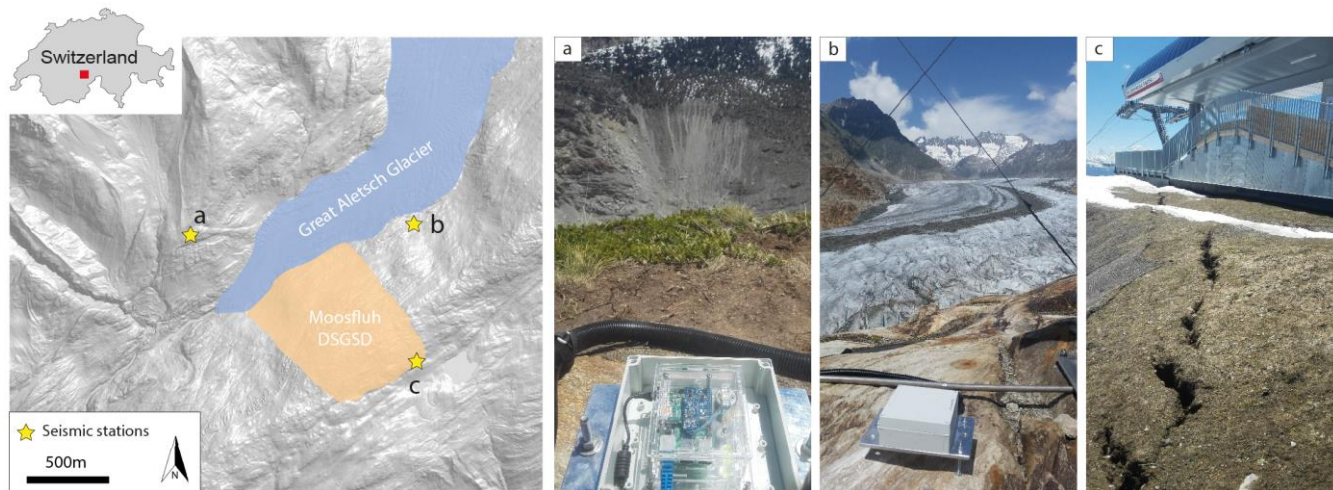
Figures

Figure 1: (left) Map of the area of investigation with indication of the location of the three RS seismic station installed starting
from May 2017. (a-c) Pictures of the RS installation (a, RS-1; b, RS-2; c, RS-3). Continuous records of seismic signals on the 3
stations are available since beginning of July 2017.
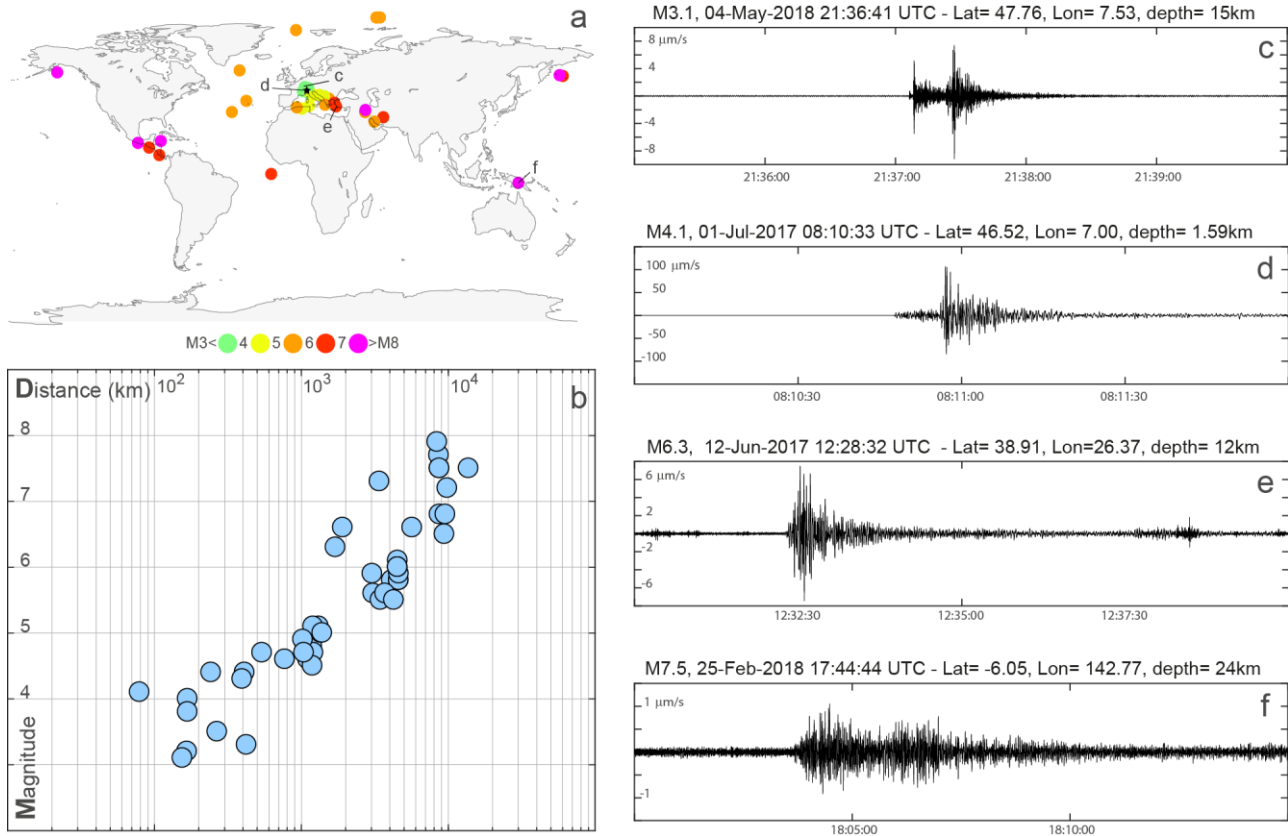
Figure 2: Performance of the RS-1 station in recording earthquakes. (a) Spatial distribution of the 47 events detected by the RS-1 among 65 selected earthquakes occurred within 1-year time period at distances up to 15,000 km from the recording station. (b) The plot shows how the probability of detecting earthquakes of lower magnitudes with RS-1 decreases when the distance from the source increases. (c-f) Examples of seismic signal recorded by RS-1 associated to earthquakes of different magnitudes and occurred at increasing distances from the monitoring station. Signals are band-pass filtered (Butterworth) between 0.5 and 15 Hz.
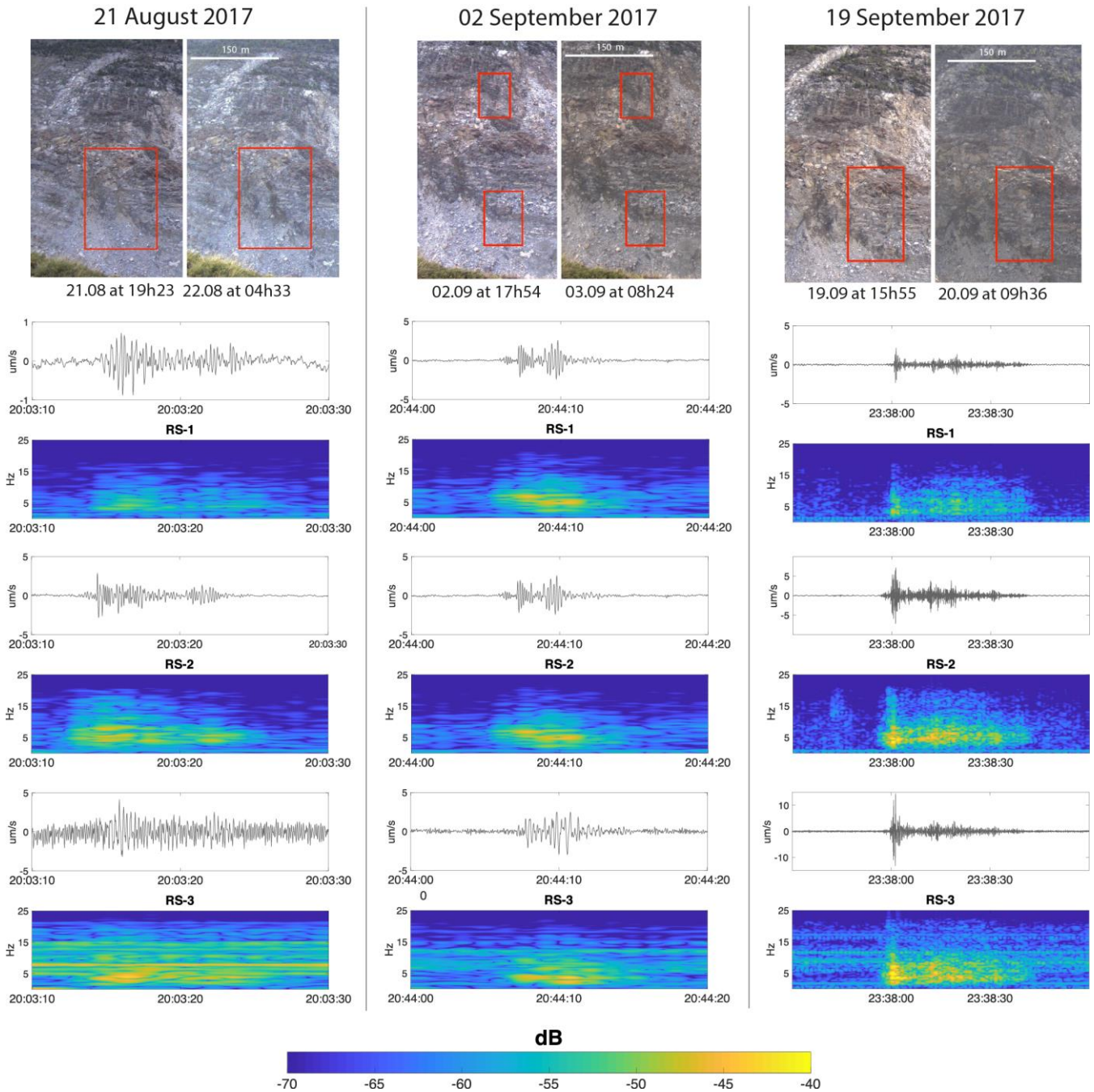
Figure 3: Selection of signals associated to rock fall events. Signals are band-pass filtered (Butterworth) between 0.5 and 15 Hz Time is in UTC. Note the large noise level at the station RS-3 caused by the cable car operations mainly during the day of 21 august 2017. Pictures acquired from the webcam before and after are shown at the top of each event. Red rectangles indicate locations of rock fall events in the imaged slope area.
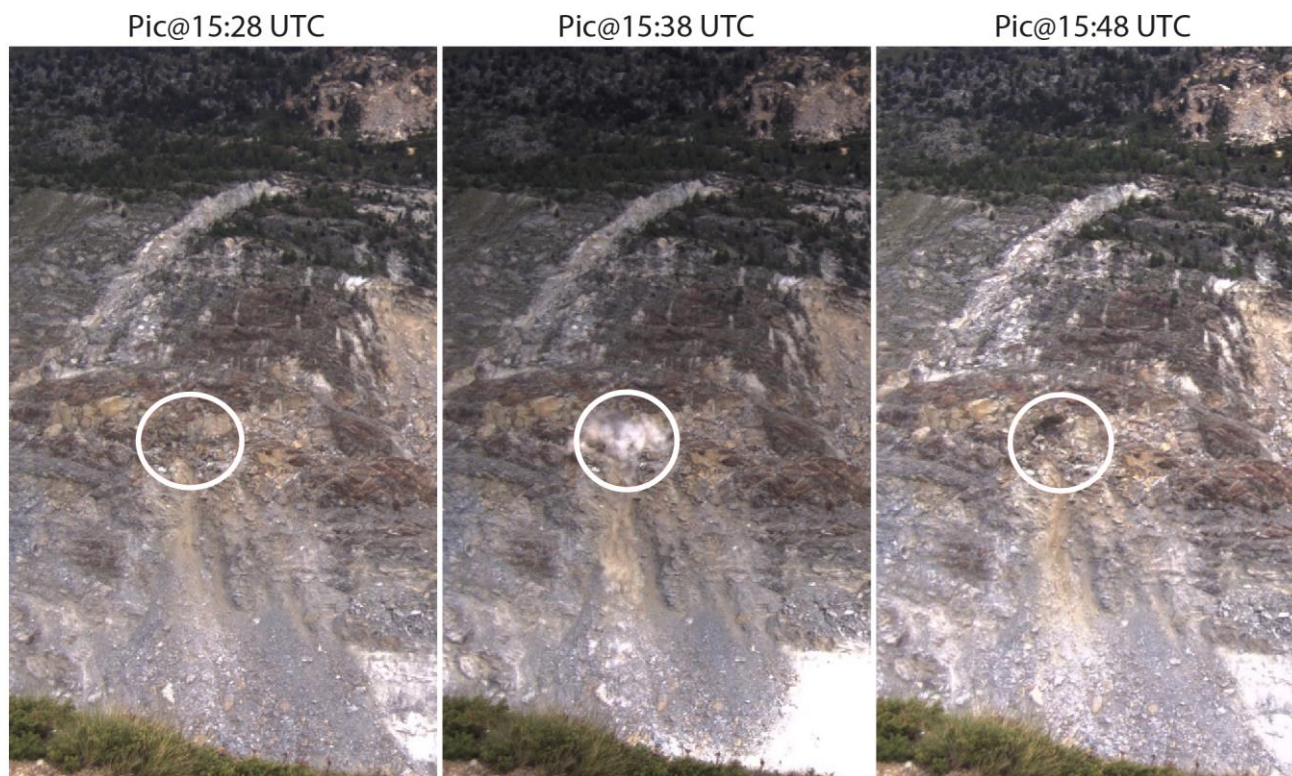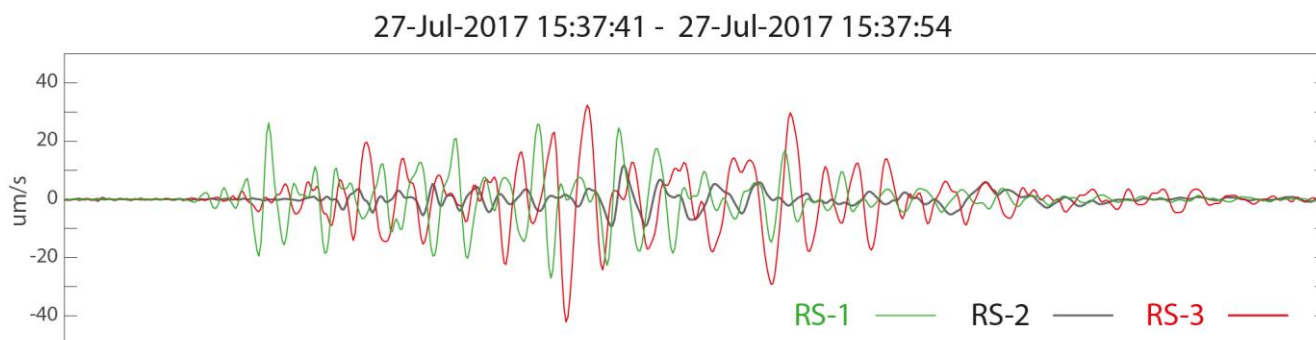
Figure 4: Detail of a rock fall event occurred on July 27, 2017 around 15:37 UTC. (Top) Seismic signal is clearly visible at the three RS stations. Note the differences in amplitudes and phases. (Bottom) Three snapshots with 10 minutes baseline acquired by the webcam. The rock fall event is clearly visible (white circle). Future work will jointly exploit seismic and optical images to locate and characterize rock fall events.